The Cryosphere Discuss., 6, 1307–1336, 2012
www.the-cryosphere-discuss.net/6/1307/2012/
doi:10.5194/tcd-6-1307-2012

The Cryosphere Discussions

Simulating the growth of supra-glacial lakes at the western margin of the Greenland ice sheet

A. A. Leeson[1], A. Shepherd[1], S. Palmer[1,*], A. Sundal[1], and X. Fettweis[2]

[1]School of Earth and Environment, University of Leeds, Leeds, LS2 9JT, UK
[2]Department of Geography, University of Liege, 4000 Liege, Belgium
[*]now at: Scott Polar Research Institute, University of Cambridge, UK

Received: 2 March 2012 – Accepted: 19 March 2012 – Published: 30 March 2012

Correspondence to: A. A. Leeson (a.leeson@see.leeds.ac.uk)

Published by Copernicus Publications on behalf of the European Geosciences Union.

Abstract

We present a method of modelling the growth of supra-glacial lakes at the western margin of the Greenland ice sheet, based on routeing runoff estimated by a Regional Climate Model (RCM) across a digital elevation model (DEM) of the ice sheet surface. Using data acquired during the 2003 melt season, we demonstrate that the model is 18 times more likely to correctly predict the presence or absence of lakes identified in MODIS satellite imagery within an elevation range of 1000 to 1600 metres above sea level (m.a.s.l.) than it is to make incorrect predictions. Our model does not, however, simulate processes leading to lake stagnation or decay, such as refreezing or drainage – a process which affects approximately 17 % of lakes in our study area (Selmes et al., 2011). This likely explains much of why our model over-predicts cumulative area by 32 % although other factors including uncertainty in the DEM and in the MODIS derived observations used for validation contribute to this error. Simulated lake filling tends to lead observations by approximately 5 days which could be related to a filling period required to saturate cracks, crevasses and other porous space within the ice. We find that the maximum modelled lake covered ice sheet area is 6 % and suggest that this is a topographic limitation for this sector. We can take this as an upper bound; given the absence of drainage in the model. In 2003, the difference between RCM estimates of runoff and the maximum volume of water simulated to be stored in lakes was 12.49 km^3. This can be taken as a measure of potential water available for lubrication and is calculated to be 1.86 m^3 per square metre of ice. This study has proved a good first step towards capturing the variability of supra-glacial lake evolution with a numerical model; we are optimistic that the model will develop further into a useful tool for use in analysing the behaviour of supra-glacial lakes on the Greenland ice sheet in the present day and beyond.

TCD

6, 1307–1336, 2012

1 Introduction

Supra-glacial lakes (SGLs) have been observed to form during the summer melt season across much of the ablation zone of the Greenland ice sheet (GrIS) (McMillan et al., 2007; Sundal et al., 2009; Sneed and Hamilton, 2007a; Selmes et al., 2011). Observations show that they form in the same locations each year (Echelmeyer et al., 1991; Selmes et al., 2011) in depressions that are controlled by the underlying bedrock topography and by spatial variations in the degree of basal ice lubrication (Gudmundsson, 2003). Runoff, a combination of melted surface snow and ice and wet precipitation, flows over the ice and through firn to areas of lower hydraulic potential. Prior to being routed off the ice sheet and into the surrounding ocean, this water may collect in supra-glacial lakes. Model studies have suggested that the area covered by supra-glacial lakes is controlled by surface topography (Luthje et al., 2006).

Supra-glacial lakes impact upon the mass balance of the ice sheet in several different ways; melt ponds have been shown to reduce the albedo of large areas of ice (Perovich et al., 2002), thereby promoting additional melting. They are also temporary water storage sites, which can modify the rate at which runoff leaves the ice sheet. At later stages of the melting season, a proportion of supra-glacial lakes drain rapidly (Selmes et al., 2011) as a result of hydro-fracture, presumably once a critical lake volume has been reached (Krawczynski et al., 2009; van der Veen, 2007) while others drain continuously at slow rates. Rapid supra-glacial lake drainage, which can occur over periods as short as a few hours, has been observed to affect short term increase in the flow velocity of the ice sheet (Das et al., 2008; Sole, 2011), and to precede seasonal increases in the rate of ice flow (Shepherd et al., 2009). It is believed that draining lakes provide a mechanism by which this occurs through opening up conduits to the base of the ice sheet and delivering large amounts of water to lubricate flow (Joughin et al., 2008; Zwally et al., 2002). This leads to a third mechanism through which ice sheet mass balance may be altered, because changes in the flow of ice can lead to changes in ablation, through modified hypsometry. Observations and model studies have shown that

TCD
6, 1307–1336, 2012

an increase in melt water supply to the ice bed results in a more efficient sub glacial drainage system, which can offset this speedup (Schoof, 2010; Sundal et al., 2011) however short term spikes in water supply, such as from the drainage of supra-glacial lakes, can lead to short term, high magnitude, velocity increases even after this efficient drainage system has been established (Bartholomew et al., 2011; Schoof, 2010). It has been suggested that in a warming climate, these short-term velocity variations will propagate further inland due to the increased abundance of melt water (Sole, 2011; Bartholomew et al., 2011) which could result in a net acceleration.

Supra-glacial lakes on the surface of the Greenland ice sheet have been surveyed using a variety of satellite imagery (e.g. Sundal et al., 2009; McMillan et al., 2007; Georgiou et al., 2009; Selmes et al., 2011; Sneed and Hamilton, 2007a). These satellite data are, however, sparsely distributed in time relative to the period over which lakes are typically present. Knowledge of supra-glacial lake evolution over shorter time periods would be of benefit for pinpointing the timing of and conditions required for lake drainage.

Here, we present a model of seasonal SGL evolution applied to the western margin of the GrIS. The model combines a digital elevation model (DEM) with a hydraulic flow model to route and pond surface water runoff estimated using the MAR (Modèle Atmosphérique Régional) regional climate model (RCM). We discuss the model performance in so far as it is able to describe the growth of SGLs, and we analyse the model sensitivity with respect to temporal resolution. Finally we extend the study to incorporate later melt seasons (2005–2007) to assess the model's capacity to represent inter-annual variability in supra-glacial lake evolution.

2 Study area and data

The model domain is restricted to a 16 000 km^2 region of western Greenland for which fine spatial resolution elevation data are available (Palmer et al., 2011), and which incorporates much of the Russell glacier catchment (Fig. 1). In this region, the ice sheet elevation ranges from 53 metres above sea level (m.a.s.l.) to 1752 m a.s.l. This entire region experiences temperatures above freezing during the ablation season, leading to abundant melting and runoff.

We use a DEM derived from interferometric synthetic aperture radar (InSAR) data acquired by the European Remote Sensing satellites in 1996 (Palmer et al., 2011) as the basis of our scheme for routeing water across the ice sheet surface. The DEM uses the Universal Transverse Mercator (UTM) projection system and is posted at a grid resolution of 100 m. We use this as our reference projection, and translate all other datasets into the same coordinate system. We geolocate the DEM using the UTM and a DEM covering the whole of Greenland (Bamber et al., 2001) to ensure accurate spatial referencing. Based on a comparison with airborne laser altimeter data, it has been estimated that DEMs formed from repeat pass InSAR data achieve a relative accuracy of between 2.5 and 10.0 m, depending upon the length of the perpendicular baseline of the interferometric SAR data (Joughin et al., 1996). In the present example, the DEM we use was formed with a perpendicular baseline of 120.0 m, and we estimate the relative accuracy to be 10.0 m. Although radar elevation measurements correspond to horizons at depth relative to the ice sheet surface due to penetration of the microwave signal into the snowpack, a study of InSAR derived topography has demonstrated that it follows that of the ice sheet surface (Rignot et al., 2001) because topography is strongly correlated with basal conditions that are transmitted through the ice (Gudmundsson, 2003), and so we are able to use this product to approximate surface topography. Large topographic gradients exist in the DEM at the data coverage margin which arise as an artefact of smoothing performed during DEM derivation. We minimise the impact of these gradients on our model by removing all cells which exhibit gradients that differ by more than one standard deviation from the local mean. This removes a margin of 1–3 cells around the ice edge only.

We use estimates of surface runoff derived from a daily product of the MAR RCM (Fettweis, 2007; Fettweis et al., 2011) run at 25 km resolution for Greenland and forced at its boundaries by the ERA-Interim reanalysis. For this study, we principally use runoff

TCD
6, 1307–1336, 2012

estimates produced for the year 2003 because this is the year for which the most complete time-series of satellite observations of lakes in this area is available for comparison. MAR is a dynamic downscaling RCM, which takes a limited geographical area at fine spatial and temporal resolution and embeds it in a global General Circulation Model (GCM) on a coarse grid/timescale. Atmospheric conditions such as temperature and pressure at the boundary of the RCM are prescribed every 6 model hours by the GCM, and additional physics is employed to downscale these data to a finer spatial and temporal resolution. The runoff product provided by the MAR model has been calculated using a snow and ice melt model which accounts for retention, percolation and refreezing of melt-water (Lefebre et al., 2003). Although runoff from MAR has not been explicitly validated due to lack of observations, the annual MAR simulated surface mass balance (precipitation – runoff) has been successfully compared to independent observations acquired over the period 1990–2011 along a transect located in the study area (Tedesco et al., 2011). In addition, Fettweis et al. (2011) have shown that the daily melt extent simulated by MAR compares well with that derived from satellite data over the period 1979–2009. The MAR data is re-projected and oversampled to the model domain before being supplied to the surface for routeing.

We use observations of supra-glacial lake area derived from MODIS satellite imagery to assess the skill of the model in predicting their locations and area. Observed changes in the area of 492 supra-glacial lakes were determined using an automated classification of cloud-free MODIS images acquired on 28 separate days during the 2003 summer melt season, and 13 separate days during the seasons of 2005–2007 (Sundal et al., 2009). The spatial resolution of the MODIS instrument is 250 m, and supra-glacial lakes of smaller area than this are therefore not resolved. It is estimated that supra-glacial lake area is underestimated by 12 % when using the relatively coarse-resolution MODIS data, as compared to a manual classification of fine-resolution (15 m) ASTER Imagery. There is also an error associated with the mis-categorisation of ice-covered lakes as bare ice using this automated classification method (Sundal et al., 2009). Based on a single case study, Sundal et al. (2009) suggest that this could be

TCD
6, 1307–1336, 2012

around 14.9 %. To facilitate the comparison between simulated and observed lakes, we re-projected the distribution of observed lakes on each date into the model domain.

MODIS observations are not available for 1996, the year during which the InSAR data from which the DEM was formed were acquired, however, since surface topography is strongly controlled by basal conditions (Gudmundsson, 2003), we assume a low degree of inter-annual variability in the surface topography and use this DEM to represent the ice sheet surface in the period 2003–2007. This assumption is supported by the findings of (Echelmeyer et al., 1991) and (Selmes et al., 2011) who observed that supra-glacial lakes occur in the same locations year on year.

3 Method

We employ a dynamical model of water flow based on Manning's equation for open channel flow (Manning, 1891) to simulate the evolution of SGL's on the surface of the GrIS. The 121.7 km by 131.5 km study area is represented on a model grid of square cells of length 100 m. The model first calculates flow direction on the surface, and subsequently calculates water displacement between cells for a given time-step using Manning's equation. Lake depth is calculated on a daily basis after the last time-step of the day. In the standard version of the model, the time-step is 1 min.

The direction of water flow within each model grid cell is calculated at the beginning of each time-step, and is defined as being towards the neighbouring cell whose free surface (ice surface plus lake plus free water) elevation is lowest with respect to the reference cell. If the cell itself is the lowest lying, then it is designated a "sink" to be potentially filled with water. At each time-step, an amount of the daily runoff produced from MAR, proportional to the time-step in seconds, is added to the free water in each cell. If a cell contains free water and it is a sink, water becomes incorporated into a "lake" up to the point where the cell is no longer a sink (i.e. when one of its neighbours has a lower lying free surface). If a cell contains free water and is not a sink, the flux

(Q) between the cell and its destination is calculated thus:

$$Q = Av \tag{1}$$

where A is the cross sectional area of flow, given by the difference between the maximum free water surface and the maximum lake surface, or ice surface if no lake is present, multiplied by the cell width. The water velocity v is calculated using Manning's formula for open channel flow (Manning, 1891):

$$v = \frac{1}{n} R_\mathrm{h}^{\frac{2}{3}} S^{\frac{1}{2}} \tag{2}$$

where S is the gradient of the free surface (ice surface plus lake plus free water, if present) and n is the Manning co-efficient accounting for channel friction, derived experimentally and taken here to be 0.011 for ice (Lotter, 1932). R_h is the hydraulic radius, calculated as:

$$R_\mathrm{h} = \frac{A}{L + 2d_{i,j}} \tag{3}$$

where L is the cell width and $d_{i,j}$ is the depth of runoff in the cell. The flux is divided by the area of the grid cell to get the equivalent depth of water, D, displaced per second::

$$D = \frac{Av}{L^2} \tag{4}$$

D is multiplied by t; the number of seconds in the time step (usually 60) to obtain the amount of runoff (in metres of depth) transferred at this time step. This is then added to the depth of free water present in the destination cell. Once the flow of water has been calculated at all cells, the model progresses to the next time-step.

At the end of each model day, the lake depth is calculated by subtracting the baseline ice surface elevation from the new lake surface, which is equal to the height of the ice surface plus that of the lake. This process is illustrated in Fig. 2: at time $t = 0$ the three cells all have water present, cell (b) is a sink and cells (a) and (c) flow into (b). At time

TCD
6, 1307–1336, 2012

$t = 60$ s the lake surface at (b), z_b^1, is given by $z_\mathrm{b}^0 + d_\mathrm{b}^0$ and the new depth of free water given by $\frac{v_\mathrm{a}^0 \times t \times d_\mathrm{a}^0 + v_\mathrm{c}^0 \times t \times d_\mathrm{c}^0}{L} + d_\mathrm{b}^0$. The new surface and depth of free water at (a) and (c) can be calculated in a similar manner.

Using this method all sinks are filled, including those which are practically too small to be lakes. To minimise this misclassification of small sinks as lakes, we filter out lakes which do not have at least one cell completely surrounded by other "lake" cells in our reporting of daily lake area.

We employed a steady-state version of the lake formation model to investigate the model dependence on runoff production rate from MAR. This steady-state version of the model differs from the dynamic version in that the flux of water is not calculated explicitly; instead, the accumulation of water in lakes is simulated iteratively. At the start of each model day, daily runoff generated by the MAR model is applied instantly to the ice sheet surface. For each subsequent iteration, the direction of water flow is then calculated in the same manner as the dynamic version of the model. Water deposited into sinks is incorporated into the lake surface; water deposited into cells that are not sinks is moved to the appropriate destination cell. This iterative sequence of events is then repeated to effectively simulate the flow of the water under gravity until it reaches hydraulic equilibrium. Once all of the water has either been incorporated into a lake or has run off the ice sheet, the model advances to the next model day. The lake surface is extracted each day, and small sinks of water filtered out using the same method as in the dynamic version by omitting "lakes" which are smaller than a nine cell square.

We do not model the rapid drainage of lakes, although slow lateral seepage and overspill is inherently included in this method. Knowledge of the conditions required to promote rapid drainage is limited (Selmes et al., 2011) and so it is not appropriate to attempt to parameterise it at this time.

We performed a sensitivity analysis to investigate the extent to which the performance of the dynamical model was dependent upon the characteristics of the forcing (runoff) data, including it's temporal resolution and absolute value. In order to test the model sensitivity to temporal resolution, we modified the dynamic version of the model to run in increments of 10, 60, and 600 s, respectively, and we compared the performance of the model at each resolution and the steady-state model with satellite observations. We also assessed the model sensitivity to runoff amount, because the runoff produced by MAR has not been explicitly validated. To do this, we ran the model with runoff equal to fixed fractions of that estimated by MAR. We compared the model results for each of these sensitivity experiments to observations of lake location, area and filling rates determined from the MODIS satellite dataset.

4 Results

We assess the skill of the model in predicting lake locations using two different metrics; the "odds ratio" and the Peirce skill score. Our implementation of the odds ratio approach, which was initially suggested by Stephenson (2000), follows the example of Stuber et al. (2006). We take a cellular approach and define the odds ratio as being the ratio of the odds of successfully predicting that a cell is a lake (a hit) or not (a correct rejection) to the odds of predicting a cell to be a lake cell when it is not observed to be so (a false alarm) and the odds of predicting a cell to be a non-lake cell when it is observed to contain a lake (a miss). Since the odds ratio can be positively skewed by a low event to non event ratio (Stephenson, 2000) i.e. in this case where there are many more cells with no lake than cells with lake, we also calculate the Peirce skill score (PSS; also known as the Hanssen-Kuiper Skill Score or True Skill Statistic). The PSS is a measure of accuracy described by the difference between the hit and false alarm rates and has a range of −1 to 1, with 0 representing no difference between the hit rate and false alarm rate and hence, no skill. We also compute the statistical significance of the two metrics at the 99.5 percentile.

The number of simulated lake hits (predicted and observed), false alarms (predicted but not observed), misses (observed but not forecast) and correct rejections (neither predicted nor forecast) for 2003, the year during which the sampling of the satellite observations is most dense, are presented in the form of a contingency table (Table 1). Using these data, the odds ratio is found to be 18, and so it is 18 times more likely that the lake model correctly predicts the presence or absence of a lake in a cell than it incorrectly predicts. This is found to be statistically significant at the 99.5 percentile. We calculate the PSS of our model to be 0.4 implying that our model has a useful degree of skill despite the large event to non event ratio evident in this simulation. This figure has also been found to be significant at the 99.5 percentile.

To further assess the extent to which the model is able to consistently locate lakes, we mapped the distribution of observed and simulated lakes. Figure 3a shows a comparison between observed and simulated lakes, with coincident lake area highlighted in blue. In addition to lake hits, there are simulated and observed lakes that are in close proximity, but that are not coincident. There are also a number of incidences of one simulated lake coinciding with several observed lakes. In general we see good agreement between the model and observations in terms of locating lakes, especially between elevations of 1000 and 1600 m a.s.l. Below 1000 m a.s.l., there is little agreement between the locations of simulated and observed lakes. Figure 3b also shows selected (modelled) lake bed and surface profiles, showing that the DEM is able to represent the short period wavelengths in the ice sheet surface necessary for lake formation.

We investigated the extent to which the dynamic model run at 60 s resolution was able to reproduce the temporal evolution of supra-glacial lakes. Figure 4a shows a comparison between simulated and observed daily lake area within three discrete altitude bands; 1000 to 1200 m a.s.l., 1200 to 1400 m a.s.l., and 1400 to 1600 m a.s.l. Satellite observations show that lakes initially form at lower altitudes, and subsequently form progressively further inland over the course of the melt season (Sundal et al., 2009; McMillan et al., 2007; Sneed and Hamilton, 2007b). In the MODIS dataset presented here (Fig. 4a), this pattern can also be seen. While this pattern is reproduced by the dynamic model, simulated lakes do begin to appear slightly earlier than observed lakes. In 2003, for example, simulated lakes are observed to appear as early as day

TCD
6, 1307–1336, 2012

120; however, significant growth in their area does not begin until around day 150. From this date forwards, simulated lakes appear 5, 0, and 10 days earlier than observed within the 1000 to 1200 m.a.s.l., 1200 to 1400 m a.s.l., and 1400 to 1600 m a.s.l. elevation bands, respectively. Across the combined region between 1000 and 1600 m a.s.l., the average lag time between simulated and observed lake appearance is 5 days.

The simulated lake filling rate, defined as the rate at which the lakes fill from empty to their maximum achieved area, are very similar to observed filling rates (Fig. 4b), although it is clear that the observed lakes lag the modelled lakes by 5 days.

Since the processes of lake drainage and refreezing are not incorporated within our model at this time, our results are restricted to comparisons of lake filling and are meaningful only until the date of drainage/commencement of refreezing. We can investigate model skill in simulating cumulative lake area (assuming no drainage) however, by comparing model output for daily lake area with an estimate of cumulative lake area derived from the satellite observations (Fig. 4a). The model is observed to predict the cumulative area of lakes reasonably well, with an overestimation of 51 % of the maximum lake area within the 1000 to 1200 m a.s.l. altitude band, and a 29 % overestimation within both the 1200 to 1400 m a.s.l. and 1400 to 1600 m a.s.l. altitude bands. The maximum area occupied by lakes is reached around day 202 (20 July) in both the simulated and observed cumulative lake area; about one week later than the maximum daily runoff amount in the MAR data which occurs at day 196.

Although our model does not include drainage, it is reasonable to conclude that runoff extraneous to that ponding in lakes as at the observed date of drainage or refreezing has passed into the ice sheet though englacial channels (e.g. crevasses or moulins). Between 1000 m a.s.l. and 1600 m a.s.l., up to the date of observed and simulated maximum cumulative lake area (day 202), 7.03 km^3 of runoff is produced, according to the MAR model, of which 24 % is simulated to be stored in lakes. 17 % of total runoff is estimated to be stored in observed lakes when considering a cumulative lake area and the median modelled lake cell depth of 3.11 m which gives a reasonable agreement with the simulation. Total runoff produced by MAR in 2003 for this region is 14.20 km^3 and the maximum volume of water simulated to be stored in lakes is 1.73 km^3. We assess the sensitivity of the model to the temporal resolution of the model, in order to identify the optimal configuration. There is little difference in the model skill at locating lakes when operated at different temporal resolutions. As temporal resolution varies, the odds ratio is found to be 19 when run at ten second resolution, 17 when run in steady-state mode, and 18 when run at all other resolutions. A slight decrease in PSS is observed as the temporal resolution increases, decreasing from 0.43 when run in steady-state mode to 0.39 when run at a temporal resolution of ten seconds. As temporal resolution increases, there is a corresponding increase in the agreement between simulated and observed maximum cumulative lake area. This agreement is greatest when the model is run with a temporal resolution of 10 s, overestimating maximum lake area by just 29 % overall. Although the model run at a 60 s time interval overestimates maximum cumulative lake area by 11% more than a one second time interval, we use the longer period configuration as it is computationally inexpensive. The lag between onset of simulated and observed lakes is the same in all versions of the model.

Because the estimated runoff data have not been independently evaluated, we tested the sensitivity of our model results to the quantity of runoff supplied using fixed fractions (2.0, 1.0, 0.75, 0.5, 0.25 and 0.1) of that predicted by MAR, and a time-step equal to 60 seconds. Again, in *locating* lakes, little variation in either the odds ratio or PSS are observed, with values ranging from 17 to 19 and 0.40 to 0.33 across the range of runoff fractions 1 to 0.1 respectively. Doubling the runoff amount, or reducing it by up to one half, has little impact on the maximum simulated lake area (Fig. 5); it remains at approximately 6 % in all cases. Reducing the runoff to 0.25 the MAR simulated value does, however, lead to a cumulative lake area growth profile that is more in line with the satellite observations, although the maximum lake area is still greater than that observed. Using only one tenth of the predicted runoff, the maximum lake area is very close to that observed; however the rate of lake growth is significantly lower. As expected, peak cumulative lake area is reached sooner when more runoff is supplied,

TCD
6, 1307–1336, 2012

occurring approximately on day 190, 202, 230 and 255 when the runoff fractions is equal to 2.0, 1.0, 0.75, and 0.5, respectively.

We ran the model at one minute resolution for 2005, 2006 and 2007 in addition to 2003 to investigate the performance of the model in capturing inter-annual variability in order to provide a more robust validation. These years were chosen because they were the years for which observations were available, using the same method as those for 2003 (Sundal et al., 2009). The model performs better in *locating* lakes in 2005, 2006 and 2007 than in 2003 (Table 2). Both the odds ratio and the PSS are higher for years other than 2003. We see an increase in the standard error of the PSS but for each year it is still found to be significant to the 99.5 % level.

We compare the cumulative lake area as a percentage of area coverage as simulated (solid) and observed (dashed) in Fig. 6. The model performs the best at predicting cumulative lake area in 2003 and overestimates significantly more in the other years considered. Although the maximum lake area is over predicted, the variability of cumulative lake area is reproduced well for 2003, 2005 and 2006; the simulated and observed cumulative area profiles show the same shape. Again we see that the observed lakes lag the simulated lakes in their onset, however with a lag of 15, 30 and 10 days, in 2005, 2006 and 2007 respectively we see a much greater gap in the appearance of simulated lakes and observed lakes in these years. 2003 and 2007 were particularly wet years with a total runoff amount over the whole of this sector of the ice sheet of 14.20 km^3 and 14.11 km^3 (Table 2) which corresponds to a daily mean runoff depth of 16.78 and 17.26 mm. 2005 and 2006 have over 30 % less runoff than the other two years at 8.32 km^3 and 9.39 km^3 respectively with 10.08 and 11.24 mm daily mean runoff.

5 Discussion

We present model simulations of supra-glacial lake evolution in the vicinity of the Russell glacier in western Greenland, and we evaluate the model results using

TCD
6, 1307–1336, 2012

contemporaneous satellite observations. We show that our model performs well in predicting supra-glacial lake locations (with a PSS of 0.4) and maximum cumulative lake area (with an overestimate of 29 %) within the 1000 m a.s.l. to 16000 m a.s.l. elevation band (approximately 70 % of the 16 000 km^2 catchment) but performs poorly below it. Crevasses are abundant at elevations below 1000 m a.s.l. in this sector of the GrIS, providing numerous avenues for melt water to drain before it pools in lakes. In addition, the InSAR DEM we use is least accurate in this area for the same reasons. The margin of the ice sheet experiences high climatic variability, primarily due to the steep elevation gradient but also due to the heterogeneity of surface albedo relative to the interior (van den Broeke et al., 2008; Wientjes, 2011). Consequently the modelled runoff data is not able to resolve topography and SMB this close to the Ice sheet margin (Franco et al., 2012). We also disregard model results above 1600 m a.s.l., even though our study area extends to 1751 m a.s.l. because the number of lakes is too small to provide a meaningful comparison. A small number of simulated lakes are displaced when compared to the satellite observations; this could occur, for example, through fluctuations in the ice surface topography during the period between the DEM and satellite surveys (1996 and 2003, respectively). In other locations, lakes are observed but not simulated; this may be due to limitations in the vertical precision of the DEM. The apparent over prediction of cumulative lake area is likely due to the missing drainage processes in the model with a possible contribution from error in the observations; this also provides an explanation for why daily lake area is not effectively predicted by the model.

Sensitivity analysis shows that, at elevations between 1000 and 1600 m a.s.l. the model results are dependent upon the model temporal resolution. We see a clear inverse relationship between the temporal resolution and the simulated maximum cumulative lake area. The amount of water displaced is proportional to the depth of runoff (Eq. 2) and, in dynamic simulations; the runoff depth applied at each time-step is proportional to the size of the time-step. The flux of water we observe in the coarse-resolution and steady-state simulations (which starts as *all* the runoff for the day) enables more water to reach topographic depressions and form lakes than is the case in the finer resolution simulations. While the coarse-resolution and steady-state simulations predict a maximum cumulative area which is much higher than that which we observe, finer temporal resolution simulations are computationally more demanding. We find the 60-s time-step to be the optimal trade off between model accuracy and computational efficiency.

We assess the ability of our model to reproduce inter-annual variations in supra-glacial lake evolution in 2003, 2005, 2006 and 2007. The model shows closest agreement with observations of cumulative lake area described by Sundal et al. (2009) (Fig. 6) in 2003. Our model predicts the maximum cumulative lake area to be similar in years with comparable runoff however observations suggest, particularly between 2003 and 2007, that this is not the case. Since there are 28 days of observations for 2003 and only 13 per year for the period 2005–2007 we suggest that the sparseness of observations in 2005–2007 relative to 2003 mean that observations in these years are not able to capture a comparable degree of variability in daily lake area, and we conclude that more dense temporal sampling is required to effectively investigate inter-annual variations. There is, however, good agreement in all four years between the simulated and observed lake locations, with a PSS of 0.4 or greater in all instances. Since we use the same DEM for each year, this supports our hypothesis that inter-annual variability of surface topography is small and confirms the findings of Echelmeyer et al. (1991) and Selmes et al. (2011) who used a range of observational techniques to investigate the inter-annual distribution of supra-glacial lakes on the GrIS. Both studies observed that supra-glacial lakes appear in the same locations on different years.

Our study shows that the location of supra-glacial lakes and the rate of lake growth show little dependence on the amount of runoff supplied to the ice sheet surface, when that amount is between half and double that predicted by MAR. For runoff fractions less that 0.5 there is clearly not enough runoff to produce a flux sufficient to allow all lakes to be filled. These experiments indicate that lakes would still form in the patterns observed under a wide range of runoff scenarios, allowing for relative uncertainty in

TCD
6, 1307–1336, 2012

the forcing data. The MAR model can, for example, overestimate the quantity of runoff due to the use of a constant bare-ice albedo (~0.45) for the entire bare ice area of the GrIS (Fettweis et al., 2011) however it is unlikely that this would be as much as 50 %. Modelled lake onset dates are earlier in the season when runoff is increased. This suggests that in high runoff years we would expect to see supra-glacial lakes appearing earlier in the season.

We compare our model estimates of lake filling rates to those observed in the MODIS observations. Modelled lake filling rates tend to lead observations by around 5 days (Fig. 4b). Since the daily variability of melt-extent simulated by the MAR model has been validated with satellite data (Fettweis et al., 2011) and that runoff in MAR has been simulated using a comprehensive snow model, we can speculate that this lag in modelled lake formation arises from the time taken to fill existing cracks and crevasses by runoff at the start of the melt season.

We use our model of supra-glacial lake evolution to estimate an upper bound for the area and volume of supra-glacial lakes situated at elevations between 1000 and 1600 m a.s.l. within our study area. Although simulated lake area peaks around day 210, runoff continues after this time (albeit with little impact on the size of simulated lakes). This implies that a limitation on maximum lake size is imposed by the local topography; lakes can only grow until depressions are brimful. This is consistent with the findings of Lüthje et al. (2006). In our study area, the local topographic setting limits supra-glacial lake area to around 6 % of the entire region irrespective of the quantity of runoff supplied. We estimate that the maximum volume of water that can be stored in supra-glacial lakes in this sector of the Greenland ice sheet is 1.73 km^3, or 12 % of all runoff produced in 2003. This suggests that the vast majority of runoff passes through or over the ice sheet without being stored temporarily in lakes. The volume of water not stored in lakes is equivalent to 1.86 m^3 per square metre of our study area. In a previous study (McMillan et al., 2007), it was estimated that 17 % of total melt water produced had been stored in lakes in the nearby Swiss Camp region of the GrIS by August, a value that is 60 % greater than the annual storage predicted by

TCD
6, 1307–1336, 2012

our model. However, runoff continues to be produced after August and, by the same date, our model predicts that 19 % of all runoff is stored in supra-glacial lakes within our catchment.

6 Conclusions

We have developed a model to simulate the growth of supra-glacial lakes in the Russell glacier catchment of the Greenland Ice Sheet. At altitudes between 1000 and 1600 m a.s.l., supra-glacial lakes are simulated in 2003 with a Peirce skill score of 0.4 when compared with contemporaneous satellite observations. The model over-predicts estimated cumulative lake area by 32 %, and simulated lake filling rates during the ∼160 day melt season are in close (within 5 days) agreement with satellite observations. Although increasing the model temporal resolution has little impact on the model skill in locating lakes, it does improve the agreement between estimates and observations of cumulative lake area (to within 29 %). Satellite observations of supra-glacial lake area are too sparse (13 per year) to allow an evaluation of the model performance in years other than 2003.

Our results confirm that the locations of supra-glacial lakes coincide with intransient depressions in the ice surface topography and, in our experiment, it was not essential to have contemporaneous surface elevation and runoff observations to predict where lakes form. The rate at which modelled supra-glacial lakes fill lags the onset of runoff by around five days; a possible explanation for this delay is the saturation period needed to fill porous space within the ice sheet before water ponds – a process that is not represented in our model. Within our study region, there appears to be a practical limit to the area occupied by modelled supra-glacial lakes (6 %) which is not exceeded in any of our experiments, even when double the estimated runoff amount is supplied. This limit is, however, a feature of our model, which only simulates lake growth. In practise, observed lake area tends to be considerably lower than this level. We estimate the amount of runoff not stored in lakes (i.e. that which passes through or over the ice sheet) to be equivalent to 1.86 m^3 per square meter of the study area.

Discussion Paper | Discussion Paper | Discussion Paper | Discussion Paper |

TCD

6, 1307–1336, 2012

Simulating supra-glacial lake growth on the Greenland ice sheet

A. A. Leeson et al.

It is important to note that our model simulates only lake growth, and does not incorporate processes leading to rapid lake drainage, which is known to be an aspect of the seasonal cycle of some lakes (Sundal et al., 2009; McMillan et al., 2007; Luthje et al., 2006; Georgiou et al., 2009). In consequence, while our model provides information about the location, filling rates, and cumulative area of supra-glacial lakes, it cannot simulate the evolution of lakes that drain. On the other hand, differences between modelled and observed lake volumes can provide useful information as to the quantity of water that has drained from lakes.

Acknowledgements. This work was supported by a PhD studentship awarded to A. L. by the NERC National Centre for Earth Observation.

References

Bamber, J. L., Layberry, R. L., and Gogineni, S.: A new ice thickness and bed data set for the Greenland ice sheet 1. Measurement, data reduction, and errors, J. Geophys. Res.-Atmos., 106, 33773–33780, 2001.

Bartholomew, I. D., Nienow, P., Sole, A., Mair, D., Cowton, T., King, M. A., and Palmer, S.: Seasonal variations in Greenland Ice Sheet motion: Inland extent and behaviour at higher elevations, Earth Planet. Sci. Lett., 307, 271–278, doi:10.1016/j.epsl.2011.04.014, 2011.

Box, J. E. and Ski, K.: Remote sounding of Greenland supraglacial melt lakes: implications for subglacial hydraulics, J. Glaciol., 53, 257–265, 2007.

Das, S. B., Joughin, I., Behn, M. D., Howat, I. M., King, M. A., Lizarralde, D., and Bhatia, M. P.: Fracture propagation to the base of the Greenland Ice Sheet during supraglacial lake drainage, Science, 320, 778–781, doi:10.1126/science.1153360, 2008.

Echelmeyer, K., Clarke, T. S., and Harrison, W. D.: Surficial glaciology of Jakobshavns Isbrae, West Greenland .1. Surface-Morphology, J. Glaciol., 37, 368–382, 1991.

Ettema, J., van den Broeke, M. R., van Meijgaard, E., van de Berg, W. J., Box, J. E., and Steffen, K.: Climate of the Greenland ice sheet using a high-resolution climate model – Part 1: Evaluation, The Cryosphere, 4, 511–527, doi:10.5194/tc-4-511-2010, 2010.

Fettweis, X.: Reconstruction of the 19792006 Greenland ice sheet surface mass balance us-

ing the regional climate model MAR, The Cryosphere, 1, 21–40, doi:10.5194/tc-1-21-2007, 2007.
Fettweis, X., Tedesco, M., van den Broeke, M., and Ettema, J.: Melting trends over the Greenland ice sheet (1958–2009) from spaceborne microwave data and regional climate models, The Cryosphere, 5, 359–375, doi:10.5194/tc-5-359-2011, 2011.
Franco, B., Fettweis, X., Lang, C., and Erpicum, M.: Impact of spatial resolution on the modelling of the Greenland ice sheet surface mass balance between 1990–2010, using the regional climate model MAR, The Cryosphere Discuss., 6, 635–672, doi:10.5194/tcd-6-635-2012, 2012.
Georgiou, S., Shepherd, A., McMillan, M., and Nienow, P.: Seasonal evolution of supraglacial lake volume from ASTER imagery, Ann. Glaciol., 50, 95–100, 2009.
Gudmundsson, G. H.: Transmission of basal variability to a glacier surface, J. Geophys. Res.-Sol. Ea., 108, 2253, doi:10.1029/2002jb002107, 2003.
Joughin, I., Winebrenner, D., Fahnestock, M., Kwok, R., and Krabill, W.: Measurement of ice-sheet topography using satellite radar interferometry, J. Glaciol., 42, 10–22, 1996.
Joughin, I., Das, S. B., King, M. A., Smith, B. E., Howat, I. M., and Moon, T.: Seasonal speedup along the western flank of the Greenland Ice Sheet, Science, 320, 781–783, doi:10.1126/science.1153288, 2008.
Krawczynski, M. J., Behn, M. D., Das, S. B., and Joughin, I.: Constraints on the lake volume required for hydro-fracture through ice sheets, Geophys. Res. Lett., 36, L10501, doi:10.1029/2008gl036765, 2009.
Lefebre, F., Gallee, H., van Ypersele, J. P., and Greuell, W.: Modeling of snow and ice melt at ETH Camp (West Greenland): A study of surface albedo, J. Geophys. Res.-Atmos., 108, 4231, doi:10.1029/2001jd001160, 2003.
Lotter, G. K.: Considerations on hydraulic design of channels with different roughness of walls, Transactions, All-Union Scientific Research Institute of Hydraulic Engineering, Leningrad, 1932.
Luthje, M., Pedersen, L. T., Reeh, N., and Greuell, W.: Modelling the evolution of supraglacial lakes on the West Greenland ice-sheet margin, J. Glaciol., 52, 608–618, 2006.
Manning, R.: On the flow of water in open channels and pipes, Transactions, Institution of Civil Engineers of Ireland, 20, 161–207, 1891.
McMillan, M., Nienow, P., Shepherd, A., Benham, T., and Sole, A.: Seasonal evolution of supra-glacial lakes on the Greenland Ice Sheet, Earth Planet. Sci. Lett., 262, 484–492,

TCD
6, 1307–1336, 2012

doi:10.1016/j.epsl.2007.08.002, 2007.
Palmer, S., Shepherd, A., Nienow, P., and Joughin, I.: Seasonal speedup of the Greenland Ice Sheet linked to routing of surface water, Earth Planet. Sci. Lett., 302, 423–428, doi:10.1016/j.epsl.2010.12.037, 2011.
Perovich, D. K., Grenfell, T. C., Light, B., and Hobbs, P. V.: Seasonal evolution of the albedo of multiyear Arctic sea ice, J. Geophys. Res.-Oceans, 107, 8044, doi:10.1029/2000jc000438, 2002.
Rignot, E., Echelmeyer, K., and Krabill, W.: Penetration depth of interferometric synthetic-aperture radar signals in snow and ice, Geophys. Res. Lett., 28, 3501–3504, doi:10.1029/2000gl012484, 2001.
Schoof, C.: Ice-sheet acceleration driven by melt supply variability, Nature, 468, 803–806, doi:10.1038/nature09618, 2010.
Selmes, N., Murray, T., and James, T. D.: Fast draining lakes on the Greenland Ice Sheet, Geophys. Res. Lett., 38, L15501, doi:10.1029/2011gl047872, 2011.
Shepherd, A., Hubbard, A., Nienow, P., King, M., McMillan, M., and Joughin, I.: Greenland ice sheet motion coupled with daily melting in late summer, Geophys. Res. Lett., 36, 4, L01501, doi:10.1029/2008gl035758, 2009.
Sneed, W. A. and Hamilton, G. S.: Evolution of melt pond volume on the surface of the Greenland Ice Sheet, Geophys. Res. Lett., 34, L03501, doi:10.1029/2006gl028697, 2007a.
Sneed, W. A. and Hamilton, G. S.: Evolution of melt pond volume on the surface of the Greenland Ice Sheet, Geophys. Res. Lett., 34, L03501, doi:10.1029/2006gl028697, 2007b.
Sole, A. J., Mair, D. W. F., Nienow, P. W., Bartholomew, I. D., King, M. A., Burke, M. J., and Joughin, I.: Seasonal speedup of a greenland marine-terminating outlet glacier forced by surface melt induced changes in subglacial hydrology, J. Geophys. Res., 116, F03014, doi:10.1029/2010jf001948, 2011.
Stephenson, D. B.: Use of the odds ratio for diagnosing forecast skill, Weather Forecast., 15, 221–232, doi:10.1175/1520-0434(2000)015<0221:uotorf>2.0.co;2, 2000.
Stuber, N., Forster, P., Radel, G., and Shine, K.: The importance of the diurnal and annual cycle of air traffic for contrail radiative forcing, Nature, 441, 864–867, doi:10.1038/nature04877, 2006.
Sundal, A. V., Shepherd, A., Nienow, P., Hanna, E., Palmer, S., and Huybrechts, P.: Evolution of supra-glacial lakes across the Greenland Ice Sheet, Remote Sens. Environ., 113, 2164–2171, doi:10.1016/j.rse.2009.05.018, 2009.

Sundal, A. V., Shepherd, A., Nienow, P., Hanna, E., Palmer, S., and Huybrechts, P.: Melt-induced speed-up of Greenland ice sheet offset by efficient subglacial drainage, Nature, 469, 522–583, doi:10.1038/nature09740, 2011.

Tedesco, M., Fettweis, X., van den Broeke, M. R., van de Wal, R. S. W., Smeets, C. J. P. P., van de Berg, W. J., Serreze, M. C., and Box, J. E.: The role of albedo and accumulation in the 2010 melting record in Greenland, Environ. Res. Lett., 6, 014005, doi:10.1088/1748-9326/6/1/014005, 2011.

van den Broeke, M., Smeets, P., Ettema, J., and Munneke, P. K.: Surface radiation balance in the ablation zone of the west Greenland ice sheet, J. Geophys. Res.-Atmos., 113, D13105, doi:10.1029/2007jd009283, 2008.

van der Veen, C. J.: Fracture propagation as means of rapidly transferring surface meltwater to the base of glaciers, Geophys. Res. Lett., 34, L01501, doi:10.1029/2006gl028385, 2007.

Wientjes, I. G. M., Van de Wal, R. S. W., Reichart, G. J., Sluijs, A., and Oerlemans, J.: Dust from the dark region in the western ablation zone of the Greenland ice sheet, The Cryosphere, 5, 589–601, doi:10.5194/tc-5-589-2011, 2011.

Zwally, H. J., Abdalati, W., Herring, T., Larson, K., Saba, J., and Steffen, K.: Surface melt-induced acceleration of Greenland ice-sheet flow, Science, 297, 218–222, 2002.

TCD
6, 1307–1336, 2012

Table 1. Predicted and observed lake cells in the study area.

		Lake cells observed		
		Yes	No	Total
Lake cells forecast	Yes	13 684	28 538	42 222
	No	17 106	620 673	637 779
	Total	30 790	649 211	679 830

TCD
6, 1307–1336, 2012

Table 2. Statistical description of the forecast skill in predicting lake locations in our study area between 1000 and 1600 m elevation in 2003, 2005, 2006 and 2007. Also given are the maximum observed and modelled lake areas, as a percentage of total area between 1000 and 1600 m elevation, MAR simulated runoff and the number of satellite images available for comparison with the model in each of those years. Daily mean runoff relates to the period day 130–250, which we observe to be the period during which supra-glacial lakes are seen in this sector of the GrIS.

Multi year comparison				
Year	2003	2005	2006	2007
Total runoff (km^3)	14.20	8.32	9.39	14.11
Daily average runoff (mm)	16.78	10.08	11.24	17.26
Number of satellite images available	28	13	13	13
Odds ratio	18	18	20	18
PSS	0.4	0.41	0.44	0.43
PSS standard error	0.0028	0.0037	0.0037	0.0042
Maximum modelled lake area (%)	6.21	5.68	5.95	6.22
Maximum observed lake area (%)	4.53	2.70	2.68	2.08

TCD
6, 1307–1336, 2012

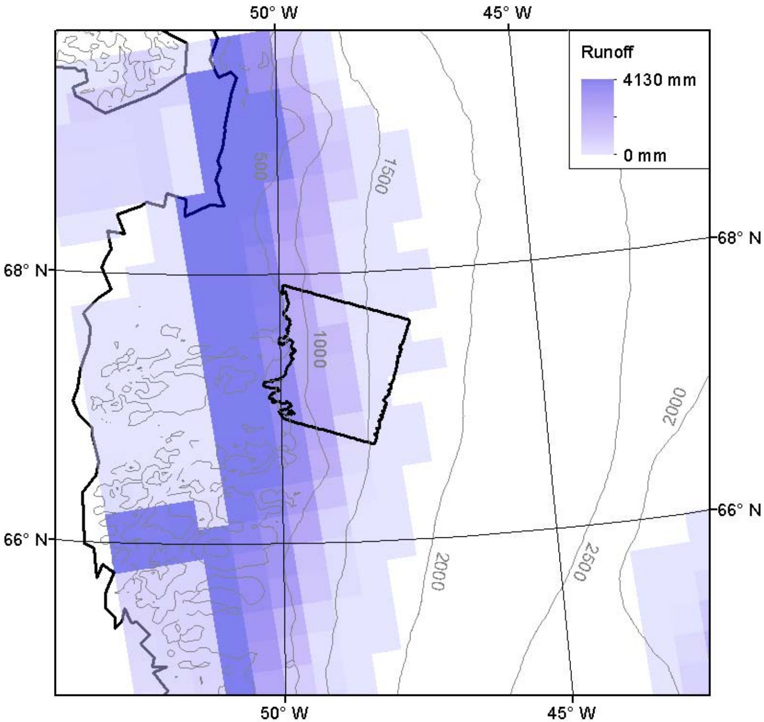

Fig. 1. Map of Greenland showing elevation contours (Bamber, Layberry et al., 2001) at 500 m intervals from 500 m. MAR simulated total runoff for 2003 is shown in blue (white areas represent zero runoff) and the DEM used in this study is bounded in black.

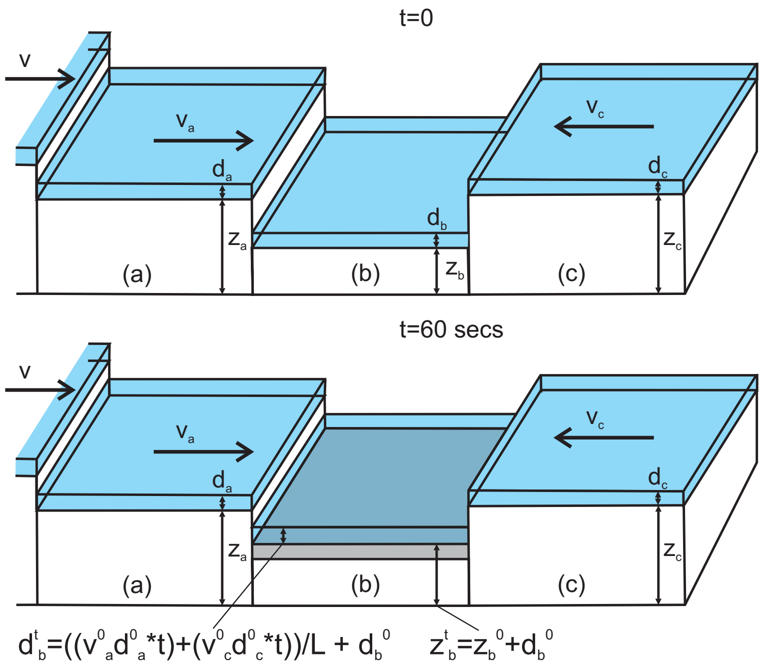

Fig. 2. 2-D representation of model processes including a sink cell (b). (Top) state of model at time $t = 0$, a layer of MAR simulated runoff covers each cell. (Bottom) state of model at time $t = 60$ s (one standard time step); the sink cell (b) now has a lake surface and each cell contains a combination of runoff from contributing cells and 86 400/(time step) of the MAR simulated daily runoff for that cell.

TCD
6, 1307–1336, 2012

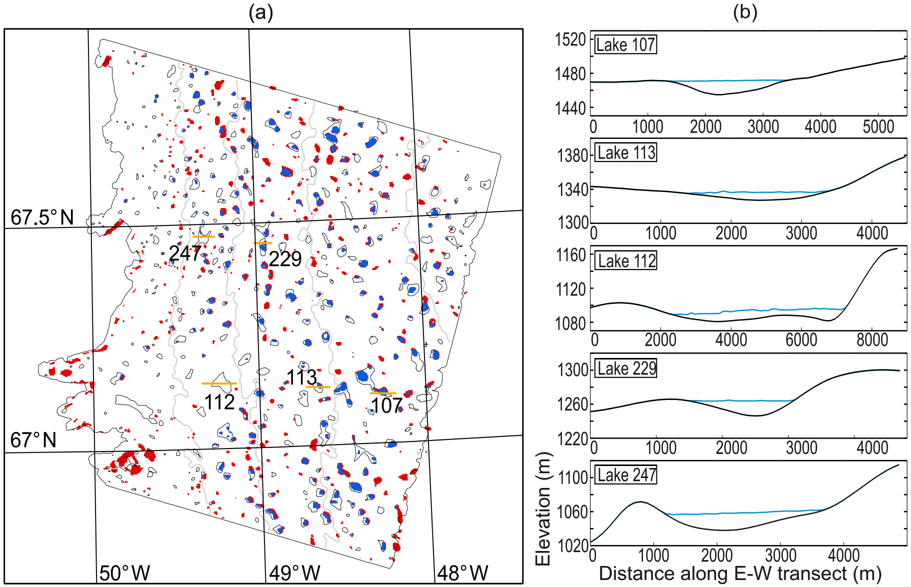

Fig. 3. (a) Composite plot of all MODIS observed lakes (red) and all lakes simulated using the dynamic version of the model (white) at a 60 s resolution for the 2003 melt season. Coincident lake area is shown in blue. **(b)** East-west lake surface (blue) and bed (solid black) profiles for modelled lakes indicated by number in the main plot. The transect taken is shown in orange in **(a)**.

TCD
6, 1307–1336, 2012

Simulating supra-glacial lake growth on the Greenland ice sheet

A. A. Leeson et al.

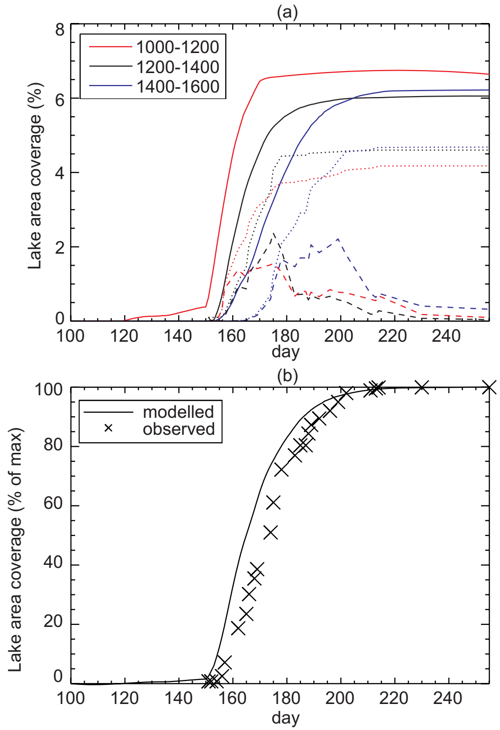

Fig. 4. (a) Comparison between modelled (solid) observed (dashed) and cumulative observed (dotted) fractional lake area for three altitude bands; we see a clear progression up the ice sheet in both modelled and observed lake area. **(b)** Comparison between modelled (solid) and observed (symbol) filling rates for lakes located between 1000 and 1600 m. A five day lag between the evolution of the modelled and observed lakes can clearly be seen.

TCD
6, 1307–1336, 2012

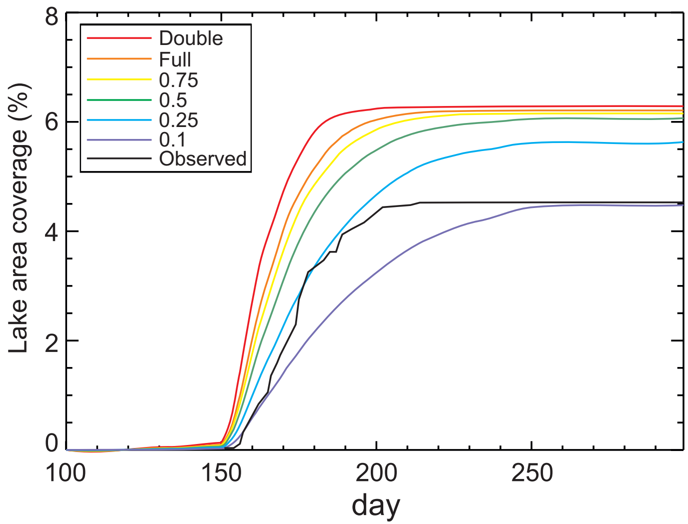

Fig. 5. Sensitivity analysis with respect to runoff amount for the 1000–1600 m elevation band of cumulative lake area. Presented here are cumulative lake area profiles simulated using the full runoff amount and proportions of 2, 0.75, 0.5, 0.25 and 0.1.

TCD
6, 1307–1336, 2012

Simulating supra-glacial lake growth on the Greenland ice sheet

A. A. Leeson et al.

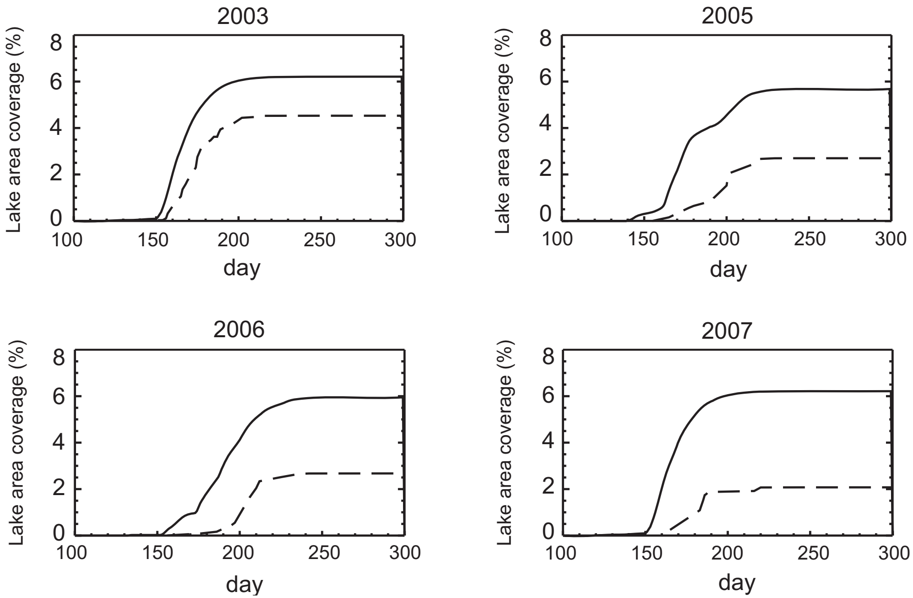

Fig. 6. Multi year comparison of cumulative lake area (1000–1600 m elevation band) as a percentage of total area. Modelled values are given with solid lines and observed values are given dashed.

TCD
6, 1307–1336, 2012

Simulating supra-glacial lake growth on the Greenland ice sheet

A. A. Leeson et al.